Supporting Information

Designing high-performance n-type Mg_3Sb_2-based thermoelectric materials through forming solid solution and biaxial strain

Juan Li, Shuai Zhang, Boyi Wang, Shichao Liu, Luo Yue, Guiwu Lu and Shuqi Zheng*

State Key Laboratory of Heavy Oil Processing, College of New Energy and Materials, China University of Petroleum, Beijing 102249, People's Republic of China

Supplementary Figures

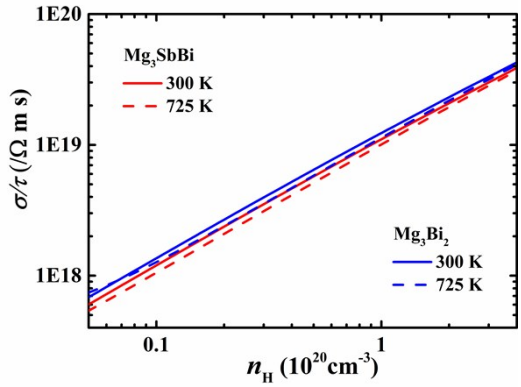

Fig. S1 Calculated electrical conductivity σ/τ as a function of Hall carrier concentration for Mg_3SbBi (red lines) and Mg_3Bi_2 (blue lines), respectively at 300 K (solid lines) and 725 K (dash lines).

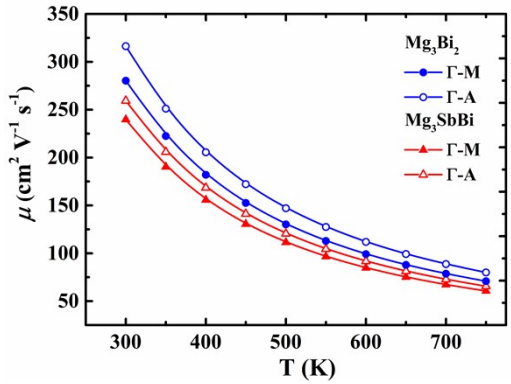

* Corresponding author. Tel: +86 010 89733200; Fax: +86 010 89733973.
E-mail: zhengsq09@163.com (Shuqi Zheng).

Fig. S2 Temperature dependence of the carrier mobility μ for Mg_3SbBi (red triangles) and Mg_3Bi_2 (blue circulars). Hollow and solid points represent the simulated results along Γ – M direction and Γ – A direction, respectively. The solid lines represent fitted curves using a *B* spline.

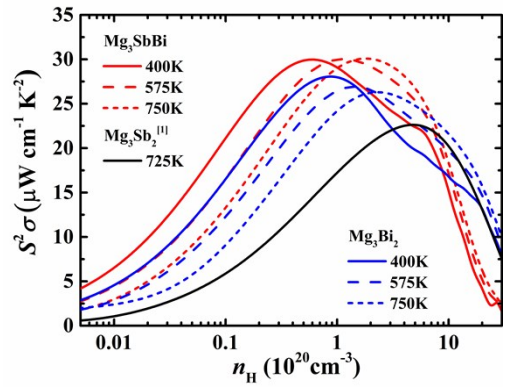

Fig. S3 Calculated power factor $S^2\sigma$ as a function of Hall carrier concentration for Mg_3SbBi (red lines) and Mg_3Bi_2 (blue lines), respectively at 400 K (solid lines), 575 K (dash lines) and 725 K (short dash lines), and the comparison with the reported Mg_3Sb_2[1] (black line).

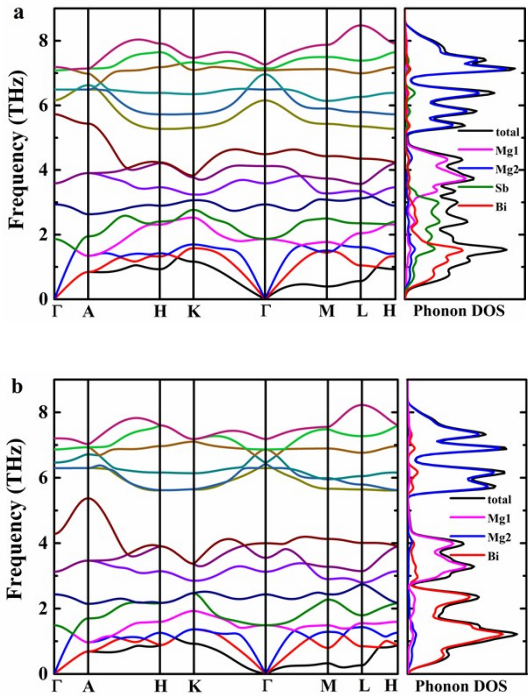

Fig. S4 Calculated phonon spectra and DOS of (a) Mg_3SbBi and (b) Mg_3Bi_2.

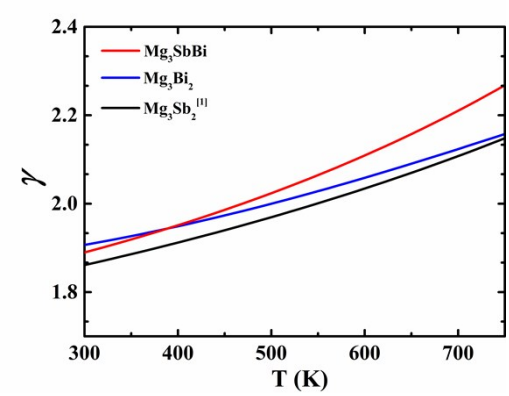

Fig. S5 Temperature dependence of the Grüneisen parameters of Mg_3SbBi and Mg_3Bi_2 and the comparison with Mg_3Sb_2.[1]

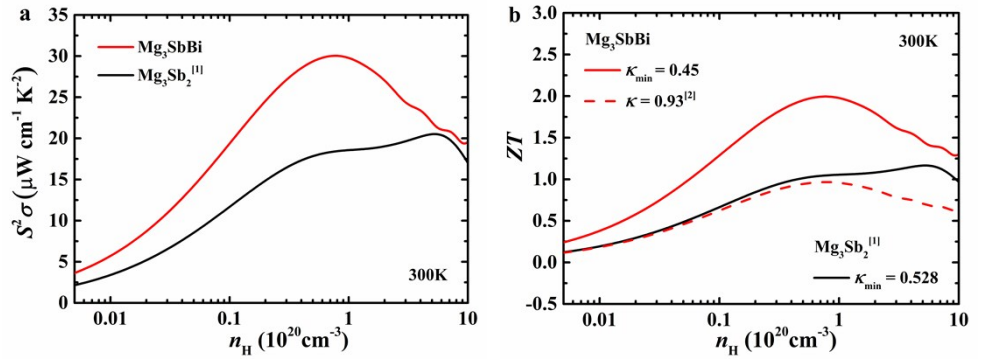

Fig. S6 (a) Calculated power factor $S^2\sigma$ and (b) ZT values versus Hall carrier concentration at 300 K for Mg_3SbBi (red lines). In (b), the dash and solid red lines represent the simulated ZT by using the experimental total thermal conductivity (W m^{-1} K^{-1}) from ref. 2 and the calculated minimum thermal conductivity (W m^{-1} K^{-1}), respectively. In (a) and (b), the reported n-type Mg_3Sb_2[1] at 300 K (black lines) are plotted for comparison.

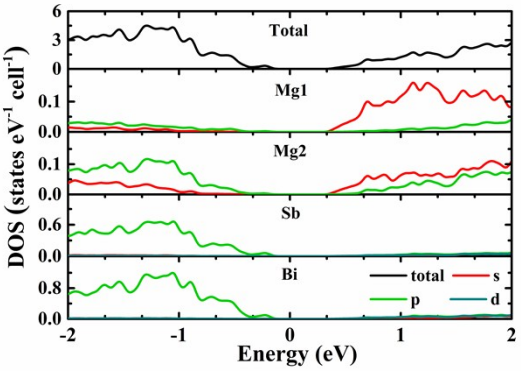

Fig. S7 Calculated total and partial DOS of Mg_3SbBi.

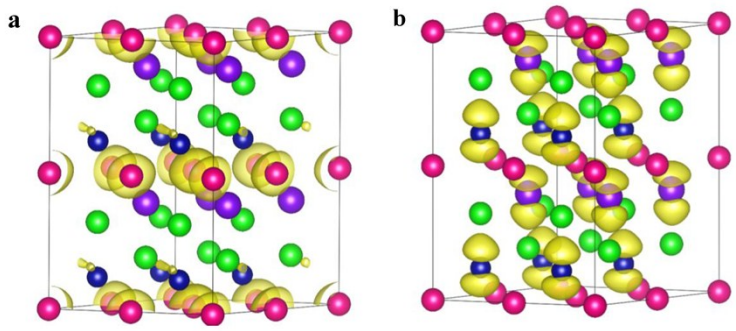

Fig. S8 Calculated band-decomposed charge density of (a) conduction band minimum (CBM), isosurface value 0.0008, and (b) valence band maximum (VBM), isosurface value 0.0008. Pink, green, blue and purple balls represent Mg1, Mg2, Sb and Bi atoms, respectively.

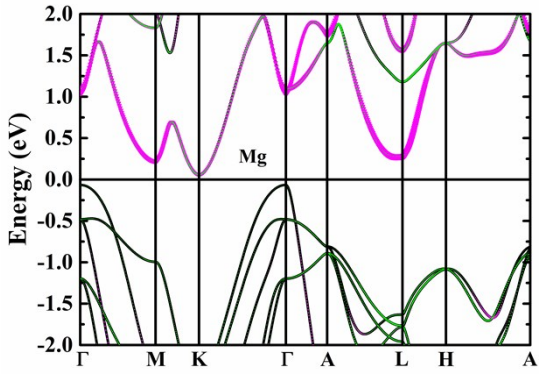

Fig. S9 Orbital-projected band structure of the Mg atom of Mg_3Sb_2. The magenta and green points represent s and p orbitals, respectively.

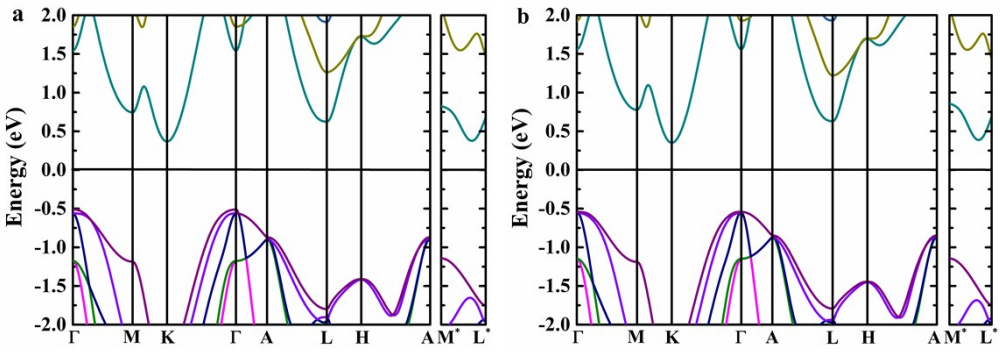

Fig. S10 Electronic band structures with (a) biaxial strain -2.5% ($\Delta E_{K\text{-}CB_1} \approx 0$) and (b) biaxial strain -3% ($\Delta E_{\Gamma} \approx 0$) for Mg_3Sb_2.

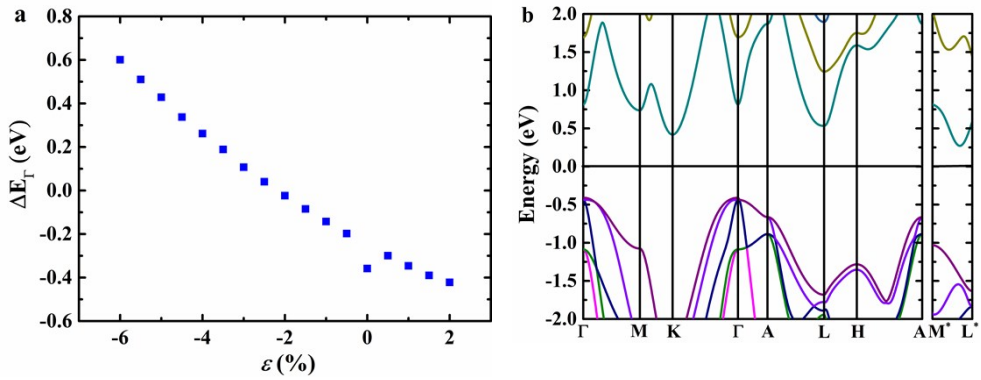

Fig. S11 (a) The energy difference ΔE_Γ between $\Gamma(p_{x,y})$ band and $\Gamma(p_z)$ band versus biaxial strain ε in Mg_3SbBi. (b) Electronic band structure with nearly zero ΔE_Γ at biaxial strain -2% in Mg_3SbBi.

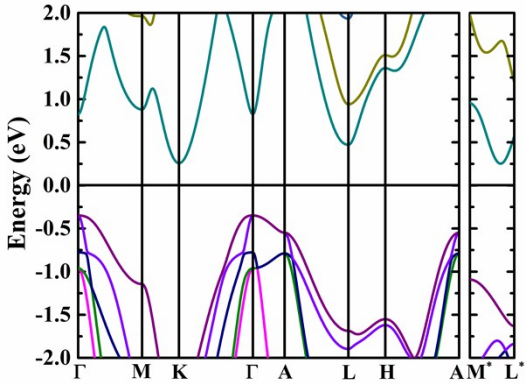

Fig. S12 Electronic band structure with nearly zero $\Delta E_{K\text{-}CB_1}$ at biaxial strain -5% in Mg_3SbBi.

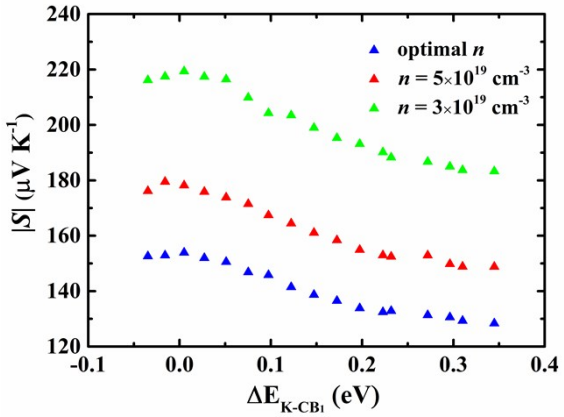

Fig. S13 Calculated absolute value of Seebeck coefficient $|S|$ of Mg_3SbBi at 300 K as a function of the energy difference $\Delta E_{K\text{-}CB_1}$ at varying carrier concentrations.

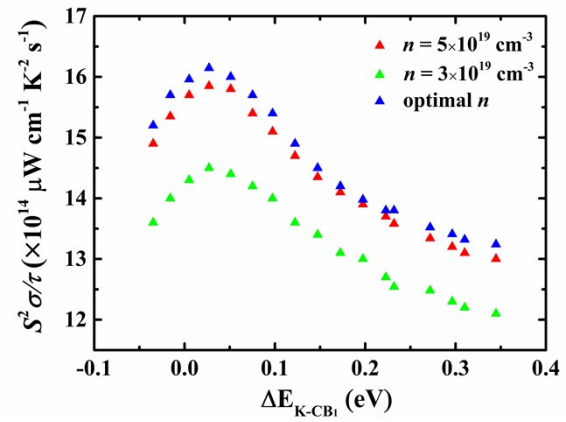

Fig. S14 Calculated power factor $S^2\sigma/\tau$ of Mg_3SbBi at 300 K as a function of $\Delta E_{K\text{-}CB_i}$ at varying carrier concentrations.

Supplementary Table

Table S1 Calculated electronic and thermal transport parameters for Mg_3SbBi and Mg_3Bi_2.

Parameters	**Mg_3SbBi**	**Mg_3Bi_2**
Lattice constant a (Å)	4.608 (4.608[a])	4.666 (4.666[b])
c (Å)	7.315 (7.315[a])	7.401 (7.401[b])
Band gap (eV)	0.4447	0.30941(0.15[c], 0.2520[d])
Effective mass (m_{xx}/m_e, m_{yy}/m_e, m_{zz}/m_e) at CB_1	(0.446, 0.13, 0.107)	(0.424, 0.115, 0.094)
Valley degeneracy of the conduction band CB_1	6	6
Valley degeneracy of the conduction band K	2	2
DOS effective mass m_d^* (m_e) of the conduction band CB_1	0.6171	0.5481
Conductivity effective mass m_1^* (m_e) of the conduction band CB_1	0.1588	0.1383
Lattice elastic constants c_{11} (GPa)	71.78963	62.49606 (64.2689[e])
Lattice elastic constants c_{33} (GPa)	77.67787	70.54759 (103.64855[e])
Lattice elastic constants c_{44} (GPa)	15.94614	12.68754 (4.0415[e])
Lattice elastic constants c_{12} (GPa)	36.60094	33.83294 (36.59395[e])
Lattice elastic constants c_{13} (GPa)	22.06376	21.25815 (39.53735[e])
Lattice elastic constants c_{66} (GPa)	13.397369	9.36672
Deformation potential constant Ξ (eV)	42.70515	43.8
Carrier mobility μ ($cm^2\ V^{-1}\ s^{-1}$) along Γ–M/ Γ–A direction at 300 K	239.697/259.357	280.240/316.344
Carrier mobility μ ($cm^2\ V^{-1}\ s^{-1}$) along Γ–M/ Γ–A direction at 725 K	63.802/69.036	74.60/84.21
Relaxation time τ ($\times 10^{-14}$ s) along Γ–M/ Γ–A direction at 300 K	2.16488/2.34245	2.19/2.488
Relaxation time τ ($\times 10^{-14}$ s) along Γ–M/ Γ–A direction at 725 K	0.57624/0.6235	0.5867/0.66239
Bulk modulus B (GPa)	42.47642	38.67821
Shear modulus G (GPa)	16.88492	13.03996
Traverse elastic wave velocity v_t ($m\ s^{-1}$)	1840.815	1494.113
Longitudinal elastic wave velocity v_l ($m\ s^{-1}$)	3611.459	3098.065
Minimum lattice thermal conductivity ($W\ m^{-1}\ K^{-1}$)	0.451702	0.367808 (0.366[f])

[a]ref. 3

[b]ref. 4

[c]ref. 5

[d]ref. 6

[e]ref. 7

[f]ref. 2

Supplementary Notes

Supplementary Note 1. The Slack' s expression

The lattice thermal conductivity can be estimated by Slack's formula[8]

$$\kappa_{\text{lat}} = A\frac{\overline{M}\Theta_{\text{D}}^3 V_{\text{per}}^{1/3}}{\gamma^2 n^{2/3} T} \quad (1)$$

where $\overline{M}$ is the average atomic mass, Θ_{D} is the Debye temperature, V_{per} is the volume per atom, n is the number of atoms in the primitive cell and γ is the Grüneisen parameter, and A is a physical constant $\approx 3.1 \times 10^{-6}$ if κ_{lat} is in W m^{-1} K^{-1}, $\overline{M}$ is in amu, and $V_{\text{per}}^{1/3}$ is in Å. Θ_{D} is closely related to the averaged sound velocity v_s and can be given by[9]

$$\Theta_{\text{D}} = \frac{\hbar}{k_B}(6\pi^2 n_a)^{1/3} v_s \quad (2)$$

where n_a is number density of atoms. v_s is related to the traverse elastic wave velocity v_t and the longitudinal elastic wave velocity v_l and can be written as[10]

$$v_s = \left[\frac{1}{3}\left(\frac{2}{v_t^3} + \frac{1}{v_l^3}\right)\right]^{-1/3} \quad (3)$$

$$v_t = \sqrt{\frac{G}{\rho}} \quad (4)$$

$$v_l = \sqrt{\left(B + \frac{4}{3}G\right)\Big/\rho} \quad (5)$$

where the bulk modulus B and shear modulus G can be calculated by the Voigt-Reuss-Hill averaging scheme in hexagonal system[11]

$$B = (B_V + B_R)/2 \quad (6)$$

$$G = (G_V + G_R)/2 \quad (7)$$

$$B_V = \frac{1}{9}(2(c_{11}+c_{12})+4c_{13}+c_{33}) \quad (8)$$

$$B_R = \frac{c^2}{M} \quad (9)$$

$$G_V = \frac{1}{30}(M+12c_{44}+12c_{66}) \quad (10)$$

$$G_R = \frac{5c^2c_{44}c_{66}}{2(3B_Vc_{44}c_{66}+c^2(c_{44}+c_{66}))} \quad (11)$$

$$M = c_{11}+c_{12}+2c_{33}-4c_{13} \quad (12)$$

$$c^2 = (c_{11}+c_{12})c_{33}-2c_{13}^2 \quad (13)$$

where c_{11}, c_{33}, c_{44}, c_{12} and c_{13} are five independent elastic constants in the hexagonal system.

The Grüneisen parameter γ based on the density functional perturbation theory (DFPT) and quasi-harmonic approximation (QHA) can be written as[12]

$$\gamma = \frac{3\beta BV_m}{C_V} \quad (14)$$

where β, B, and V_m are the linear thermal expansion coefficient, the bulk modulus, and the molar volume, respectively, and the isometric heat capacity C_V can be calculated by[12]

$$C_V = \sum_{n,q} k_B \left(\frac{\hbar\omega_n(q)}{k_BT}\right)^2 \frac{e^{\hbar\omega_n(q)/k_BT}}{\left(e^{\hbar\omega_n(q)/k_BT}-1\right)^2} \quad (15)$$

where $\omega_n(q)$ is the phonon frequency of the n-th branch with wave vector q. The input parameters for the calculations are shown in Table S1.

Supplementary Note 2. The Cahill's expression

The low limit of thermal conductivity is the minimum lattice thermal conductivity, which can be estimated by Cahill's formula[9]

$$\kappa_{\min} = \frac{1}{2}[(\frac{\pi}{6})^{1/3}]k_B(V)^{-2/3}(2v_t + v_l) \quad (16)$$

Where V, v_t, v_l are the average volume per atom, the traverse elastic wave velocity and the longitudinal elastic wave velocity, respectively. The calculated $\kappa_{\min}$ for Mg_3SbBi is 0.452 W m^{-1} K^{-1} and the $\kappa_{\min}$ for Mg_3Bi_2 is estimated to be 0.378 W m^{-1} K^{-1}, which is in well agreement with the previously reported value of 0.366 W m^{-1} K^{-1}.[2]

Supplementary References

1 J. Li, S. Zheng, T. Fang, L. Yue, S. Zhang and G. Lu, *Phys. Chem. Chem. Phys.*, 2018, **20**, 7686-7693.

2 H. Tamaki, H. K. Sato and T. Kanno, *Adv. Mater.*, 2016, **28**, 10182-10187.

3 K. Imasato, S. D. Kang, S. Ohno and G. J. Snyder, *Mater. Horiz.*, 2018, **5**, 59-64.

4 J. Zhang, L. Song, G. K. Madsen, K. F. Fischer, W. Zhang, X. Shi and B. B. Iversen, *Nat. Commun.*, 2016, **7**, 10892.

5 L. M. Watson, C. A. W. Marshall and C. P. Cardoso, *J. Phys. F: Met. Phys.*, 1984, **14**, 113.

6 M. Sedighi, B. A. Nia, H. Zarringhalam and R. Moradian, *Eur. Phys. J. Appl. Phys.*, 2013, **61**, 10103.

7 D. W. Zhou, J. S. Liu, S. H. Xu and P. Peng, *Physica B*, 2010, **405**, 2863–2868.

8 G. A. Slack, *J. Phys. Chem. Solids*, 1973, **34**, 321-335.

9 D. G. Cahill, S. K. Watson and P. R. Pohl, *Phys. Rev. B: Condens. Matter Mater. Phys.*, 1992, **46**, 6131-6140.

10 O. L. Anderson, *J. Phys. Chem. Solids*, 1963, **24**, 909-917.

11 Z. J. Wu, E. J. Zhao, H. P. Xiang, X. F. Hao, X. J. Liu and J. Meng, *Phys. Rev. B*, 2007, **76**, 054115.

12 T. Fang, S. Zheng, T. Zhou, L. Yan and P. Zhang, *Phys. Chem. Chem. Phys.*, 2017, **19**, 4411-4417.